

Transverse momentum dependence of directed particle flow at 160A GeV

E. E. Zabrodin^{1,2}, C. Fuchs,¹ L. V. Bravina,^{1,2} and Amand Faessler¹

¹*Institute for Theoretical Physics, University of Tübingen,
Auf der Morgenstelle 14, D-72076 Tübingen, Germany*

²*Institute for Nuclear Physics, Moscow State University, RU-119899 Moscow, Russia*

Abstract

The transverse momentum (p_t) dependence of hadron flow at SPS energies is studied. In particular, the nucleon and pion flow in S+S and Pb+Pb collisions at 160A GeV is investigated. For simulations the microscopic quark-gluon string model (QGSM) is applied. It is found that the directed flow of pions $v_1(y, \Delta p_t)$ changes sign from a negative slope in the low- p_t region to a positive slope at $p_t \geq 0.6$ GeV/ c as recently also observed experimentally. The change of the flow behaviour can be explained by early emission times for high- p_t pions. We further found that a substantial amount of high- p_t pions are produced in the very first primary NN collisions at the surface region of the touching nuclei. Thus, at SPS energies high- p_t nucleons seem to be a better probe for the hot and dense early phase of nuclear collisions than high- p_t pions. Both, in the light and in the heavy system the pion directed flow $v_1(p_t, \Delta y)$ exhibits large negative values when the transverse momentum approaches zero, as also seen experimentally in Pb+Pb collisions. It is found that this effect is caused by nuclear shadowing. The proton flow, in contrary, shows the typical linear increase with rising p_t .

PACS numbers: 25.75.-q, 25.75.Ld, 24.10.Lx, 24.10.Jv

I. INTRODUCTION

The collective flow of hadrons in ultrarelativistic heavy-ion collisions is a very useful signal to probe the evolution of hot and dense nuclear matter from the onset of its formation [1–7]. Since the development of flow is closely related to the equation of state (EOS) of nuclear matter, the investigation of the flow can shed light on the transition to a new phase of matter, the so-called quark-gluon plasma (QGP), and its subsequent hadronization [8–26]. If the transition from the QGP to hadronic phase is of first order, the vanishing of the pressure gradients in the mixed phase leads to the so-called softening of the EOS [9,10]. The latter should be distinctly seen in the behaviour of the excitation function of the collective flow.

At present, the Fourier expansion technique is widely employed to study collective flow phenomena [27–29]. Namely, the invariant distribution $E \frac{d^3N}{d^3p}$ is presented as

$$E \frac{d^3N}{d^3p} = \frac{1}{\pi} \frac{d^2N}{dp_t^2 dy} \left[1 + 2 \sum_{n=1}^{\infty} v_n \cos(n\phi) \right], \quad (1)$$

where p_t and y are the transverse momentum and rapidity, and ϕ is the azimuthal angle between the momentum of the particle and the reaction plane. The first two Fourier coefficients in Eq.(1), v_1 and v_2 , are dubbed directed and elliptic flow, respectively. Since both types of anisotropic flow depend on rapidity and transverse momentum, one is able to study double differential distributions

$$v_n(p_t, \Delta y) = \int_{y_1}^{y_2} \cos(n\phi) \frac{d^2N}{dp_t^2 dy} dy \bigg/ \int_{y_1}^{y_2} \frac{d^2N}{dp_t^2 dy} dy \quad (2)$$

and

$$v_n(y, \Delta p_t) = \int_{p_t^{(1)}}^{p_t^{(2)}} \cos(n\phi) \frac{d^2N}{dp_t^2 dy} dp_t^2 \bigg/ \int_{p_t^{(1)}}^{p_t^{(2)}} \frac{d^2N}{dp_t^2 dy} dp_t^2 . \quad (3)$$

Model calculations show that elliptic flow is built up at the early phase of nuclear collisions [13,21], whereas directed flow develops until the late stage of the reaction [30]. But it is well known that the particles with high transverse momentum are emitted at the onset of the collective expansion, i.e., their directed flow can carry information about the EOS of the dense nuclear phase. Our first goal is to check the emission times of high- p_t hadrons and to study the transverse momentum dependence of directed flow in heavy-ion collisions at SPS (160A GeV) energies.

Apparently, one would expect that the directed flow drops to zero when the transverse momentum decreases. For protons such a behaviour has been observed at SIS energies (≤ 1 AGeV) [31]. Experimental results on pion and proton directed flow at both AGS [22] and SPS [23] energies, show a qualitatively different picture: $v_1(p_t)$ is positive at high p_t and slightly but negative at low transverse momenta, i.e., it approaches zero from the negative side. One of the possible explanations of such a peculiar behaviour has been proposed in

[28] within the framework of a thermal model. Here the interplay of the radial expansion of a thermalized source and the directed flow has been discussed. It was shown that the $v_1(p_t)$ of protons became negative at small values of the transverse momentum provided the transverse expansion velocity of a thermalized source was $\beta \cong 0.55c$ or higher. However, the significance of, e.g., an initial anisotropy of the geometrical configuration in non-central collision for the development of anisotropic flow is not completely understood at energies above $10A$ GeV. The aim of the present paper is also to elaborate the role of non-dynamic, i.e. geometrical effects, which can cause the preferential emission of particles in the direction opposite to that of the normal flow (the so-called antiflow) at small p_t . For this purpose the quark-gluon string model (QGSM) [32] is chosen.

The paper is organised as follows. A brief description of the microscopic model is given in Sect. II. Rapidity and transverse momentum dependences of frozen nucleons and pions, calculated in Pb+Pb central collisions at $160A$ GeV, are also discussed. Section III presents a systematic study of the directed pion and nucleon flow at SPS energies as a function of p_t and y . A comparison with experimental data is performed as far as those are available. The directed flow of nucleons, which is developed alongside of the normal flow, grows with rising transverse momentum, while the directed flow of pions changes its orientation from antiflow at low p_t 's to normal flow at high transverse momenta. In order to compare to the predictions of the thermal approach [28] as well, the calculations for the proton flow are fitted by an expanding thermalized source. Finally, conclusions are drawn in Sect. IV.

II. FEATURES OF PARTICLE PRODUCTION AND FREEZE-OUT IN THE MODEL

The QGSM, which treats the elementary hadronic interactions on the basis of Gribov-Regge theory, is based on the $1/N_c$ (where N_c is the number of quark colours or flavours) topological expansion of the amplitude for processes in quantum chromodynamics and string phenomenology of particle production in inelastic binary collisions of hadrons. The model incorporates the production of particles via string excitation and subsequent fragmentation, as well as the formation of resonances and hadron rescattering. As independent degrees of freedom the QGSM includes octet and nonet vector and pseudoscalar mesons, and octet and decuplet baryons, and their antiparticles. The model simplifies the in-medium effects and focuses mainly on the development of an intranuclear cascade. Further details on the QGSM can be found elsewhere [32].

For the simulations at SPS energies, $E_{lab} = 160A$ GeV, light $^{32}\text{S}+^{32}\text{S}$ and heavy $^{208}\text{Pb}+^{208}\text{Pb}$ symmetric systems have been chosen. According to the QGSM predictions [33] the mean number of interactions per hadron, $\langle N_{int}^h \rangle$, equals 2 even for central sulphur-sulphur collisions and 9 for central lead-lead collisions at $160A$ GeV. Due to a significant increase of $\langle N_{int}^h \rangle$ with rising mass number, one can study the role of the intranuclear cascade on the formation of transverse collective flow. Although the light S+S system, or rather a part of it, cannot be treated as a thermalized source, the formation of thermally equilibrated matter in Pb+Pb collisions is not ruled out. The system expands until all interactions and decays in the reaction have ceased. This stage corresponds to the conditions of the thermal freeze-out. Note also that the system of final particles in the course of model simulations may be well approximated by a core and a halo structure. The halo contains frozen particles

already decoupled from the main system, and the core consists of hadrons intensively interacting, both elastically and inelastically, with each other. In other words, there is no sharp freeze-out picture in the microscopic model like the QGSM [33] or the relativistic quantum molecular dynamics (RQMD) model [34], in contrast to macroscopic hydrodynamic models (see, e.g., [35,36] and references therein).

The evolution of the number of frozen particles with time t is shown in Fig. 1(a) for pions and nucleons in Pb+Pb central collisions. The contour plots (dashed areas) correspond to the dN/dt distribution in different rapidity intervals. One can see that the pionic distributions peak at $t \approx 8$ fm/ c , and the nucleon distributions reach their maxima later, at $t \approx 15$ fm/ c . It is interesting that the positions of the maxima on the time scale are not shifted when the rapidity range is enlarged. Many hadrons with high rapidity, especially pions, are emitted from the very beginning of the nuclear collision. These particles usually have rather high transverse momentum as well. To illustrate this idea, the time evolution of the transverse mass distributions of nucleons and pions at the freeze-out is shown in Fig. 1(b). We see that nucleons with maximal transverse momenta in lead-lead collisions are coming either from the very beginning of the reaction or from intermediate times with a maximum at $t \approx 13$ fm/ c . In contrast to nucleons pions with highest p_t are produced in inelastic primary NN collisions in heavy-ion reactions, while soft particles are emitted during the whole evolution time. This is a general trend in the production of soft and hard particles in relativistic heavy-ion collisions. Since the excitation function of the transverse particle flow is very sensitive to pressure gradients in the system, the directed flow of both pions and nucleons might change its behaviour with increasing p_t . Obviously, pions coming from primary NN collisions cannot carry information about properties of hot and dense nuclear matter, nor about the relaxation process. These particles are just produced in the surface regions of the touching nuclei. The admixture of such pions will severely distort the spectrum of pions stemming from the (nearly) thermalized source. In contrast, the fraction of high- p_t nucleons emitted promptly after the primary collisions is relatively small compared to total number of high- p_t nucleons. Therefore, the spectrum of nucleons with large transverse momentum in heavy-ion collisions at SPS energies might be even more useful to study the early stage of the fireball evolution than that of pions.

III. DIRECTED FLOW OF HADRONS

A. Comparison with experimental data

First, directed flow and elliptic flow of pions and protons, calculated for Pb+Pb minimum bias events with the maximum impact parameter $b_{max} = 11$ fm at SPS energies, are compared in Fig. 2 with the experimental data of the NA49 Collaboration [24]. Both for pions and for protons the agreement between the microscopic calculations and the experimental data, as well as with the relativistic quantum molecular dynamics (RQMD) model results (see Fig. 1 of [30]), is quite reasonable. The directed flow of protons has a positive slope in the midrapidity range, which becomes steeper as the rapidity window is shifted towards projectile/target rapidity. Also, the pionic directed flow, which has a characteristic negative slope of $v_1(y)$ in the range $1 \leq y \leq 5$, drops to zero and even becomes positive at $y \approx y_{max}$. This behaviour can be understood, provided the fast particles are formed on the leading

quarks (mesons) and diquarks (baryons) at the early times of the collision. The number of secondary interactions per particle with high rapidity is small, thus, the flow in the fragmentation regions is basically determined by the initial geometry of the system [30]. The centrality dependence of anisotropic flow in the QGSM has been studied in [37–39]. However, as was discussed in Sect. II, the directed flow of soft particles should differ from that of hard particles. Therefore, the $v_1(y, \Delta p_t)$ distribution given by Eq. (3) is used to study the transverse momentum dependence of directed flow.

B. $v_1(y)$ in p_t intervals

Figure 3 depicts the directed flow of nucleons and pions in two p_t intervals, $0.3 < p_t < 0.6$ GeV/ c and $0.6 < p_t < 0.9$ GeV/ c , for Pb+Pb collisions with different centrality. The maximum impact parameter for a symmetric system is $b_{max} = 2R_A$. The value of the reduced impact parameter $\tilde{b} = b/b_{max}$ in the simulations varies from 0.15 (central collisions) up to 0.9 (most peripheral collisions). At $p_t < 0.6$ GeV/ c the pionic flow exhibits the typical antiproton flow in both, semicentral and peripheral, collisions. In the same p_t interval the nucleon flow increases as the reaction becomes more peripheral. But at $b \approx 8$ fm the flow becomes softer in the midrapidity range. In very peripheral collisions the directed flow of nucleons shows an antiproton behaviour which is similar to that of the pionic directed flow. As was shown in [37–39], see also [30,40], such a transformation of the nucleon flow is explained merely by shadowing: It is well known that the presence of even a small amount of quark-gluon plasma leads to a softening of the equation of state, which results in a significant reduction of the directed flow. However, since the QGP is expected to be produced primarily in central heavy-ion collisions, the effect should be most pronounced in central collisions. In contrast, shadowing causes the disappearance of nucleon directed flow and the development of antiproton flow in the midrapidity region especially in semiperipheral and peripheral collisions, as well as in light systems.

The behaviour of directed flow changes drastically in the transverse momentum range $0.6 < p_t < 0.9$ GeV/ c , presented in Fig. 3(b). Although the nucleon directed flow decreases in the midrapidity range at $b \geq 10$ fm, its normal component still dominates over the antiproton counterpart. Moreover, even high- p_t pions prefer the direction of normal flow, distinctly seen in semiperipheral events with $4 \leq b \leq 6$ fm. This reflects again that hadrons with high transverse momenta ($p_t \geq 0.6$ GeV/ c) are produced mainly at the early stage of nuclear collisions, as was discussed in Sect. II, see Fig. 1(b).

The transition of the directed flow of pions from antiproton flow to normal flow with rising transverse momentum has recently been observed in Au+Au collisions at 1 AGeV [41]. The effect is stronger in peripheral collisions and at target rapidities. Likely, this can be explained by the effective shadowing caused by the spectator matter, in accord with quantum molecular dynamics (QMD) transport calculations. A similar feature is seen at SPS at projectile rapidities (see below). However, there is a difference in correlations between early freeze-out times and high transverse momentum of hadrons in heavy-ion collisions at 1A GeV and 160A GeV: At 1A GeV high- p_t pions are emitted within the first 15-20 fm/ c of the reaction [42–44] and can be used as a “time clock” for the reaction which probes the high density phase [41]. However, at SIS energies high- p_t pions have experienced in average more than two reactions by the formation and subsequent decay of Δ -resonances [42], which is enough

for at least partial thermalization of their spectrum. In contrast to this, high- p_t pions as a probe of the hot and dense phase in Pb+Pb collisions at 160A GeV should be handled with care because of the lack of rescattering for extremely energetic pions in the latter case.

The role of rescattering in the formation of directed flow is illustrated in Fig. 4. Here the directed flow as a function of rapidity in several p_t intervals is compared in minimum bias S+S and Pb+Pb events at 160A GeV. Lacking a sufficiently large amount of secondary interactions per hadron, the directed flow of both nucleons and pions in the light S+S system varies very weakly with rising transverse momentum from $p_t \leq 0.3$ GeV/ c to $0.6 < p_t < 0.9$ GeV/ c . Nevertheless, the change of the slope of pionic directed flow from antiflow to normal flow with rising p_t is distinctly seen for both reactions. In the heavy ion system the directed flow of hadrons, especially nucleons, strongly depends on the p_t range. Note that, since the bulk amount of particles is produced with transverse momenta less than 300 MeV/ c , the distribution, given by Eq. (3) integrated over the whole p_t interval, is very close to that for $0 < p_t < 0.3$ GeV/ c .

C. $v_1(p_t)$ in rapidity intervals

Figure 5 depicts the directed flow of pions and nucleons as a function of their transverse momentum in different rapidity windows. Both, in S+S and Pb+Pb collisions the directed flow of nucleons weakly depends on p_t in the midrapidity range, $3 < y < 4$. It starts rising with increasing p_t near the projectile/target rapidity. The directed flow of pions seems to increase, especially in lead-lead collisions, with rising transverse momentum. At $p_t \leq 0.3$ GeV/ c the flow of pions in both reactions is small but negative in all three rapidity intervals. A similar picture is observed for low- p_t nucleons with the rapidity $y \leq 5$ in S+S collisions. As already mentioned in the introduction, one possible explanation for the occurrence of antiflow at low p_t is the collective motion of a group of particles, which are in (local) thermal equilibrium. Using the expression for the directed flow of non-relativistic particles emitted isotropically by a transversely expanding thermal source [28]:

$$v_1(p_t) = \frac{p_t \beta_a}{2T} \left[1 - \frac{m \beta_0}{p_t} \frac{I_1(\xi)}{I_0(\xi)} \right], \quad (4)$$

$$\xi = \frac{\beta_0 p_t}{T}, \quad (5)$$

where T is the temperature, β_a is the collective velocity along the directed flow axis, β_0 is the transverse expansion velocity of the source, and I is the modified Bessel function, one can also reproduce the negative values of $v_1(p_t)$ in the low p_t region. Note, that the validity of Eq. (4) for protons is restricted to the range of $p_t \leq 0.5$ GeV/ c . A relativistic generalisation of Eq. (4) to an expansion in three dimensions [28] leads to an increase of about 15% in the expansion velocity needed to describe the low p_t dip in the $v_1(p_t)$ distribution. Results for a fit of Eq. (4) to the low- p_t part ($p_t \leq 0.4$ GeV/ c) of the $v_1^N(p_t)$ distribution in the rapidity interval $4 < y < 5$ are plotted in Fig. 5 also. The fitting parameters are $\beta_a = 0.1c$, $T = 140$ MeV, and $\beta_0 = 0.60(0.40)c$ for S+S (Pb+Pb) collisions. However, the collective flow in sulphur-sulphur system is weak [8], and the whole system is far from being in thermal equilibrium. Therefore, the plausible explanation of negative values of $v_1(p_t)$ is shadowing.

It is worth noting that the flow of Δ resonances follows the nucleon flow (see, e.g., [45]). Pions coming from the decays of Δ 's behave similar to pions emitted from a moving thermal source [22], i.e., the pionic flow which originates from Δ resonance decays should be positive at high p_T and negative at low transverse momenta. Also, in lead-lead collisions local thermal equilibrium can be reached at least in the central zone of semicentral collisions with impact parameter $b \leq 4$ fm [46–48]. In such events directed flow can be affected by a radial isotropic expansion, the formation of long-lived Δ resonance matter, and nuclear shadowing. In peripheral collisions the possible formation of a thermalized source becomes less important. Here the development of nucleon antiproton flow in the midrapidity region, as well as in the low p_t interval, is completely determined by shadowing.

To compare results of the microscopic calculations with the experimental data, the directed flow of protons and pions in the rapidity range $4 < y < 5$ is shown separately in Fig. 6(a). One sees that the model describes the flow of pions reasonably well, but predicts much stronger signal for protons at $p_t \geq 0.25$ GeV/ c . In this context it should be noticed that the p_t dependence measured by the NA49 Collaboration [23] substantially deviates from the systematics seen at both SIS [31] and AGS [22] energies, where almost a linear increase of the proton directed flow with p_t has been observed in Au+Au collisions. In the latter case this behaviour is well reproduced by the RQMD simulations (see Fig. 20 of [3]). Thus, at SPS energies the QGSM predictions are in line with the SIS/AGS flow systematics, whereas the NA49 Collaboration observes almost a zero proton flow signal as a function of transverse momentum in the interval $0.1 \leq p_t \leq 0.9$ GeV/ c . The present minimum bias calculations are directly compared with the data in the corresponding rapidity window. If this comparison is not biased by (unknown to us) efficiency cuts (in [23] no special cuts were mentioned), this fact, in principle, can be taken as indication of a new dynamical feature not included into the current version of the QGSM. It is interesting that in the target fragmentation region, where, for instance, the formation of the QGP is quite unlikely, the model predictions for the directed flow $v_1^p(p_t)$ are close to the experimental data of the WA98 Collaboration [26], as shown in Fig. 6(b). But the production of even a small amount of quark-gluon plasma should reduce the strength of the low- p_t pion flow too. A few explanations which can lead to revision of the experimental data have been proposed recently [49,50]. The main argument is as follows: Whereas the orientation of the reaction plane is well defined in the microscopic calculations, its orientation in the experimental event has to be somehow reconstructed. Two-particle correlations in the azimuthal plane are usually applied for this purpose. However, as was discussed in detail in [49,50], there are several other sources of azimuthal particle correlations not related to the flow. Experimental data corrected for transverse momentum and Hanbury-Brown-Twiss (HBT) correlations for pions, and for p_t -correlations and correlations from Δ decays for protons [50], are plotted onto the results of microscopic calculations in Fig. 6(a) also. We see that the directed flow of protons is almost not changed due to substantial mutual cancellations of p_t correlations and Δ -decay correlations, working in the opposite direction. The agreement between the model calculations and corrected data for the directed flow of low- p_t pions becomes even worse. On the other hand, comparison between the VENUS [51] raw data sample and the data filtered through the GEANT model of the NA49 detector seems to reveal that the sources of non-flow correlations are insignificant [23]. This important problem, definitely, needs further investigations. It would be very interesting also to compare model predictions with the

coming data on sulphur-sulphur collisions [52].

IV. CONCLUSIONS

In summary, we have for the first time performed a systematic study of the directed flow of nucleons and pions as a function of rapidity in different p_t intervals at SPS energies. It is shown that the slope of the directed flow of nucleons with $p_t \leq 0.6$ GeV/ c is positive (normal flow) in semicentral and semiperipheral collisions, and negative (antiflow) in very peripheral ones, where $b/b_{max} \geq 0.7$. At higher transverse momenta the slopes of both, pion and nucleon directed flow become positive. Our findings agree with recent experimental results which report a change of sign for the pion directed flow with increasing p_t in Au+Au collisions at SIS energies [41]. There the effect was attributed solely to shadowing by the spectator matter. It was found also that high- p_t pions ($p_t \geq 0.4$ GeV/ c) in heavy-ion reactions at 1A GeV are emitted within the first 13 fm/ c or even earlier. The microscopic analysis of the particle freeze-out conditions in heavy-ion collisions at SPS energies shows that particles with maximal p_t are produced essentially either in primary nucleon-nucleon collisions (mesons and nucleons) or in the early phase of the reaction within the first 17 fm/ c (nucleons). In the yield of high- p_t nucleons the admixture of those emitted within the first two fm/ c 's is small. This means that high- p_t nucleons might be very useful to study the nuclear equation of state at high temperatures and densities whereas a large amount of high- p_t pions is produced even too early to probe this phase.

The pion and nucleon directed flow in S+S collisions, as well as pion directed flow in Pb+Pb collisions, indicates negative values as particle transverse momenta approach zero. Such behaviour can be explained by the interference between a radially expanded thermalized system and anisotropic flow [28]. However, since the formation of a rapidly expanding thermal source in peripheral heavy-ion collisions and in light S+S collisions is rather unlikely, the effect must be caused by nuclear shadowing. Hadrons emitted at small rapidity in the antiflow direction can propagate freely, while hadrons emitted in the normal flow direction still remain within the expanding subsystem (or core) of interacting particles. To study the interplay between the isotropic radial flow and anisotropic directed flow one has to subtract shadowing from the analysis of experimental data.

The microscopic model calculations are in reasonable agreement with most experimental data on anisotropic flow, both directed and elliptic, in minimum bias Pb+Pb events. The model is able to reproduce quantitatively the strong negative flow of pions, $v_1^\pi(p_t, 4 < y < 5)$, at low transverse momenta, $p_t \leq 0.25$ GeV/ c which is seen by the NA49 Collaboration. Concerning the p_t dependence of the proton flow the model calculations show the same systematics as observed at SIS and AGS energies, namely, a linear rise of the v_1 with p_t , whereas the very weak signal at $p_t \leq 0.9$ GeV/ c is observed in this rapidity window. If the comparison with data is not biased by unknown efficiency cuts, there is left space for the speculation about dynamical features not incorporated into the microscopic model. To clarify this point and to make more definite conclusions it would be interesting also to compare the model calculations with forthcoming S+S data at the same energy.

ACKNOWLEDGMENTS

We are thankful to L. Csernai, P. Danielewicz, D. Röhrich, D. Strottman, and H. Wolter for the interesting discussions and fruitful comments. This work was supported in part by the Bundesministerium für Bildung und Forschung (BMBF) under contract 06TÜ986.

REFERENCES

- [1] H. Stöcker and W. Greiner, Phys. Rep. **137**, 277 (1986).
- [2] W. Reisdorf and H. G. Ritter, Annu. Rev. Nucl. Part. Sci. **47**, 663 (1997).
- [3] N. Herrmann, J. P. Wessels, and T. Wienold, Annu. Rev. Nucl. Part. Sci. **49**, 581 (1999).
- [4] P. Danielewicz, Nucl. Phys. **A661**, 82c (1999).
- [5] J.-Y. Ollitrault, Phys. Rev. D **46**, 229 (1992); Nucl. Phys. **A638**, 195c (1998).
- [6] L. P. Csernai, *Introduction to Relativistic Heavy Ion Collisions*, (Wiley, Chichester, 1994).
- [7] T. Gaitanos, C. Fuchs, and H. H. Wolter, Nucl. Phys. **A650**, 97 (1999); Phys. Lett. B **381**, 23 (1996).
- [8] N. S. Amelin, E. F. Staubo, L. P. Csernai, V. D. Toneev, K. K. Gudima, and D. Strottman, Phys. Rev. Lett. **67**, 1523 (1991).
- [9] C. M. Hung and E. V. Shuryak, Phys. Rev. Lett. **75**, 4003 (1995).
- [10] D. H. Rischke and M. Gyulassy, Nucl. Phys. **A597**, 701 (1996).
- [11] L. V. Bravina, L. P. Csernai, P. Lévai, and D. Strottman, Phys. Rev. C **50**, 2161 (1994); L. V. Bravina, N. S. Amelin, L. P. Csernai, P. Lévai, and D. Strottman, Nucl. Phys. **A566**, 461c (1994).
- [12] J. Sollfrank, P. Huovinen, M. Kataja, P. V. Ruuskanen, M. Prakash, and R. Venugopalan, Phys. Rev. C **55**, 392 (1997).
- [13] H. Sorge, Phys. Lett. B **402**, 251 (1997).
- [14] H. Sorge, Phys. Rev. Lett. **78**, 2309 (1997).
- [15] H. Sorge, Phys. Rev. Lett. **82**, 2048 (1999); Nucl. Phys. **A661**, 577c (1999).
- [16] H. Heisenberg and A.-M. Levy, Phys. Rev. C **59**, 2716 (1999).
- [17] L. P. Csernai and D. Röhrich, Phys. Lett. B **458**, 454 (1999).
- [18] D. H. Rischke, Y. Pürsün, J. A. Maruhn, H. Stöcker, and W. Greiner, Heavy Ion Phys. **1**, 309 (1995).
- [19] J. Brachmann, S. Soff, A. Dumitru, H. Stöcker, J. A. Maruhn, L. V. Bravina, W. Greiner, and D. H. Rischke, Phys. Rev. C **61**, 024909 (2000).
- [20] B.-A. Li, C. M. Ko, A. T. Sushtich, and B. Zhang, Phys. Rev. C **60**, 011901 (1999).
- [21] P. F. Kolb, J. Sollfrank, and U. Heinz, Phys. Lett. B **459**, 667 (1999); hep-ph/0006129.
- [22] J. Barrette *et al.*, E877 Collab., Phys. Rev. C **56**, 3254 (1997); S. A. Voloshin for the E877 Collab., Nucl. Phys. **A638**, 455c (1998).
- [23] H. Appelshäuser *et al.*, NA49 Collab., Phys. Rev. Lett. **80** (1998) 4136.
- [24] A. M. Poskanzer and S. A. Voloshin for the NA49 Collab., Nucl. Phys. **A661**, 341c (1999).
- [25] M. M. Aggarwal *et al.*, WA98 Collab., Phys. Lett. B **469**, 30 (1999).
- [26] T. Peitzmann for the WA98 Collab., Nucl. Phys. **A661**, 191c (1999); H. Schlagheck for the WA98 Collab., *ibid.* **A661**, 337c (1999); S. Nishimura for the WA98 Collab., *ibid.* **A661**, 464c (1999).
- [27] S. Voloshin and Y. Zhang, Z. Phys. C **70**, 665 (1996).
- [28] S. A. Voloshin, Phys. Rev. C **55**, R1630 (1997).
- [29] A. M. Poskanzer and S. A. Voloshin, Phys. Rev. C **58**, 1671 (1998).
- [30] H. Liu, S. Panitkin, and N. Xu, Phys. Rev. C **59**, 348 (1999).
- [31] A. Andronic, FOPI Collab., (private communication).
- [32] N. S. Amelin, L. V. Bravina, L. I. Sarycheva, and L. N. Smirnova, Sov. J. Nucl. Phys.

- 50**, 1058 (1989);
N. S. Amelin and L. V. Bravina, Sov. J. Nucl. Phys. **51**, 133 (1990);
N. S. Amelin, L. V. Bravina, L. P. Csernai, V. D. Toneev, K. K. Gudima, and S. Yu. Sivoklokov, Phys. Rev. C **47**, 2299 (1993).
- [33] L. V. Bravina, I. N. Mishustin, J. P. Bondorf, Amand Faessler, and E. E. Zabrodin, Phys. Rev. C **60**, 044905 (1999).
- [34] H. Sorge, Phys. Lett. B **373**, 16 (1996).
- [35] V. K. Magas, C. Anderlik, L. P. Csernai, F. Grassi, W. Greiner, Y. Hama, T. Kodama, Z. I. Lazar, and H. Stöcker, Heavy Ion Phys. **9**, 193 (1999).
- [36] K. A. Bugaev, M. I. Gorenstein, and W. Greiner, J. Phys. G **25**, 2147 (1999).
- [37] L. V. Bravina, Phys. Lett. B **344**, 49 (1995).
- [38] L. V. Bravina, E. E. Zabrodin, Amand Faessler, and C. Fuchs, Phys. Lett. B **470**, 27 (1999).
- [39] L.V. Bravina, Amand Faessler, C. Fuchs, and E.E. Zabrodin, Phys. Rev. C **61**, 064902 (2000).
- [40] R. J. M. Snellings, H. Sorge, S. A. Voloshin, F. Q. Wang, and N. Xu, Phys. Rev. Lett. **84**, 2803 (2000).
- [41] A. Wagner *et al.*, Phys. Rev. Lett. **85**, 18 (2000).
- [42] S. A. Bass, C. Hartnack, H. Stöcker, and W. Greiner, Phys. Rev. Lett. **71**, 1144 (1993); Phys. Rev. C **50**, 2167 (1994).
- [43] B.-A. Li, W. Bauer, and G. F. Bertsch, Phys. Rev. C **44**, 450 (1991).
- [44] V. S. Uma Maheswari, C. Fuchs, Amand Faessler, L. Sehn, D. Kosov, and Z. Wang, Nucl. Phys. **A628**, 669 (1998).
- [45] S. A. Bass, M. Hofmann, C. Hartnack, H. Stöcker, and W. Greiner, Phys. Lett. B **335**, 289 (1994).
- [46] G. D. Yen and M. I. Gorenstein, Phys. Rev. C **59**, 2788 (1999).
- [47] L.V. Bravina, E. E. Zabrodin, M. I. Gorenstein, S. A. Bass, M. Belkacem, M. Bleicher, M. Brandstetter, C. Ernst, M. Hoffman, L. Neise, S. Soff, H. Weber, H. Stöcker, and W. Greiner, Phys. Rev. C **60**, 024904 (1999);
L. V. Bravina, M. I. Gorenstein, M. Belkacem, S. A. Bass, M. Bleicher, M. Brandstetter, M. Hoffman, S. Soff, C. Spieles, H. Weber, H. Stöcker, and W. Greiner, Phys. Lett. B **434**, 379 (1998).
- [48] J. Cleymans and K. Redlich, Phys. Rev. C **60**, 054908 (1999).
- [49] P. M. Dinh, N. Borghini, and J.-Y. Ollitrault, Phys. Lett. B **477**, 51 (2000).
- [50] N. Borghini, P. M. Dinh, and J.-Y. Ollitrault, Phys. Rev. C **62**, 034902 (2000).
- [51] K. Werner, Phys. Rep. **232**, 87 (1993).
- [52] D. Röhrich (private communication).

FIGURES

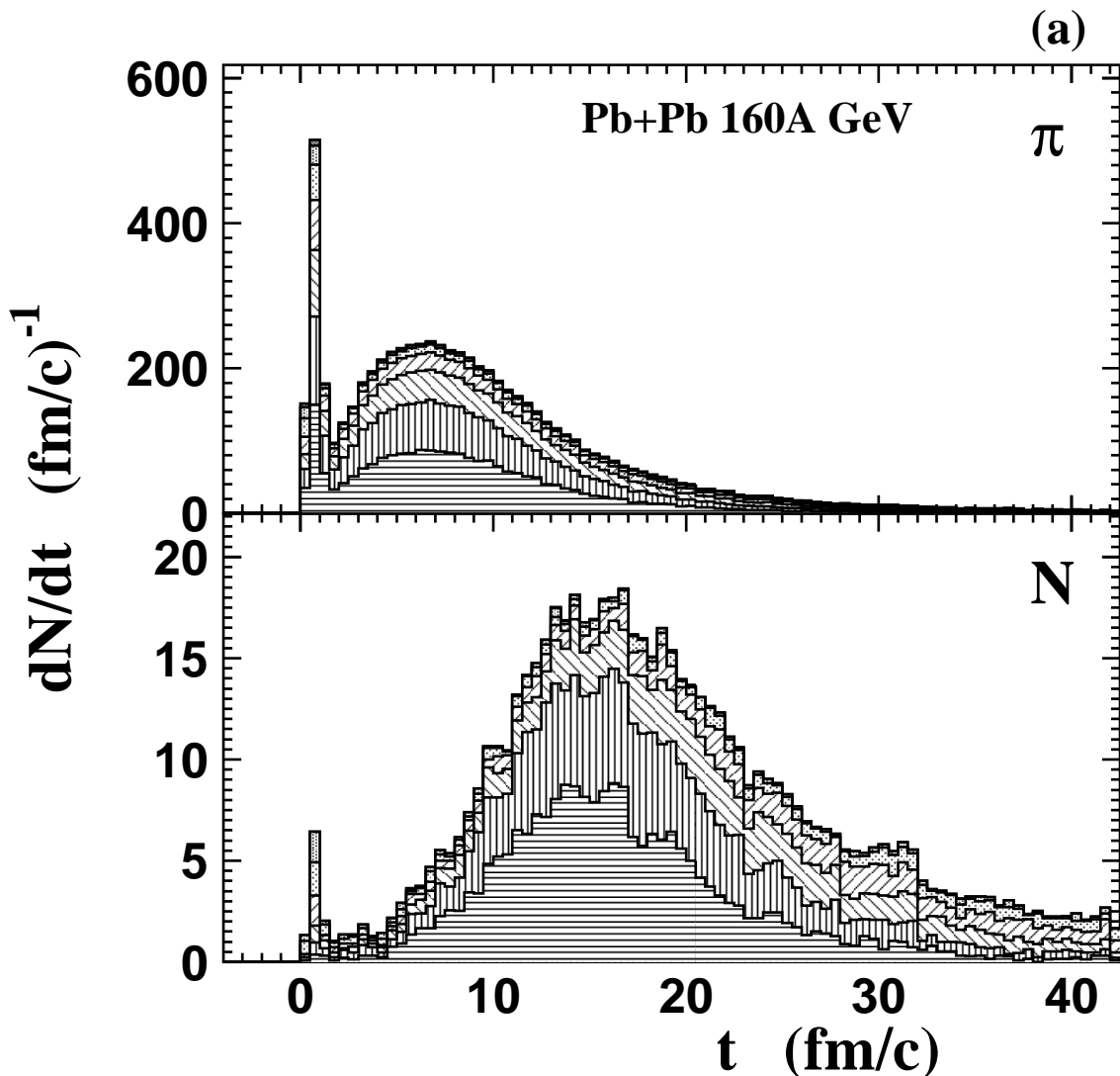
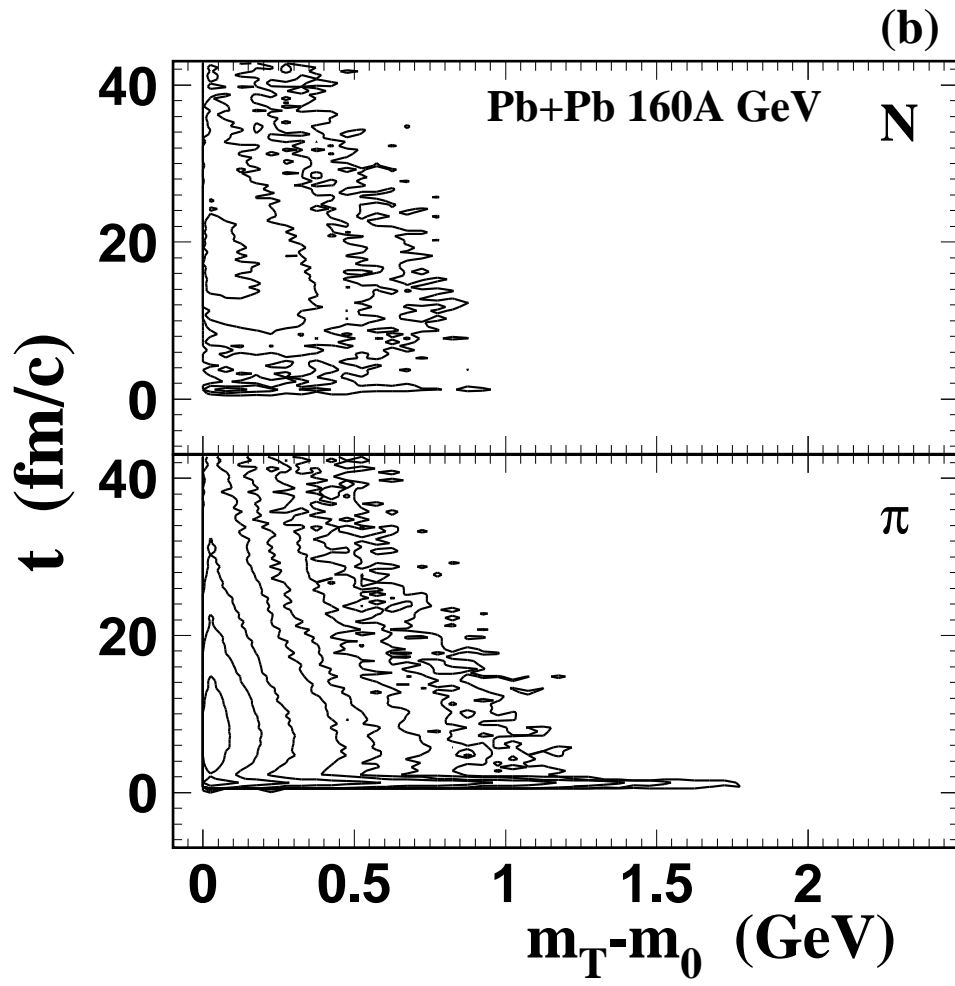


FIG. 1. (a) Evolution of number of frozen pions (upper panel) and nucleons (lower panel) with time t in central Pb+Pb collisions at 160A GeV. Hatched areas correspond to the central-mass-frame rapidity intervals $|y_{c.m.}| < 0.5, 1.0, \dots 3.5$.

(b) Transverse mass distribution $d^2N/m_T dm_T dt / A$ of the final-state nucleons (upper panel) and pions (lower panel) according to their emission time t . Contour plots correspond to densities $d^2N/m_T dm_T dt / A = 0.003, 0.01, 0.03, 0.1, 0.25, 1.0, 3.0, 10.0$ particles per fm^2/c .



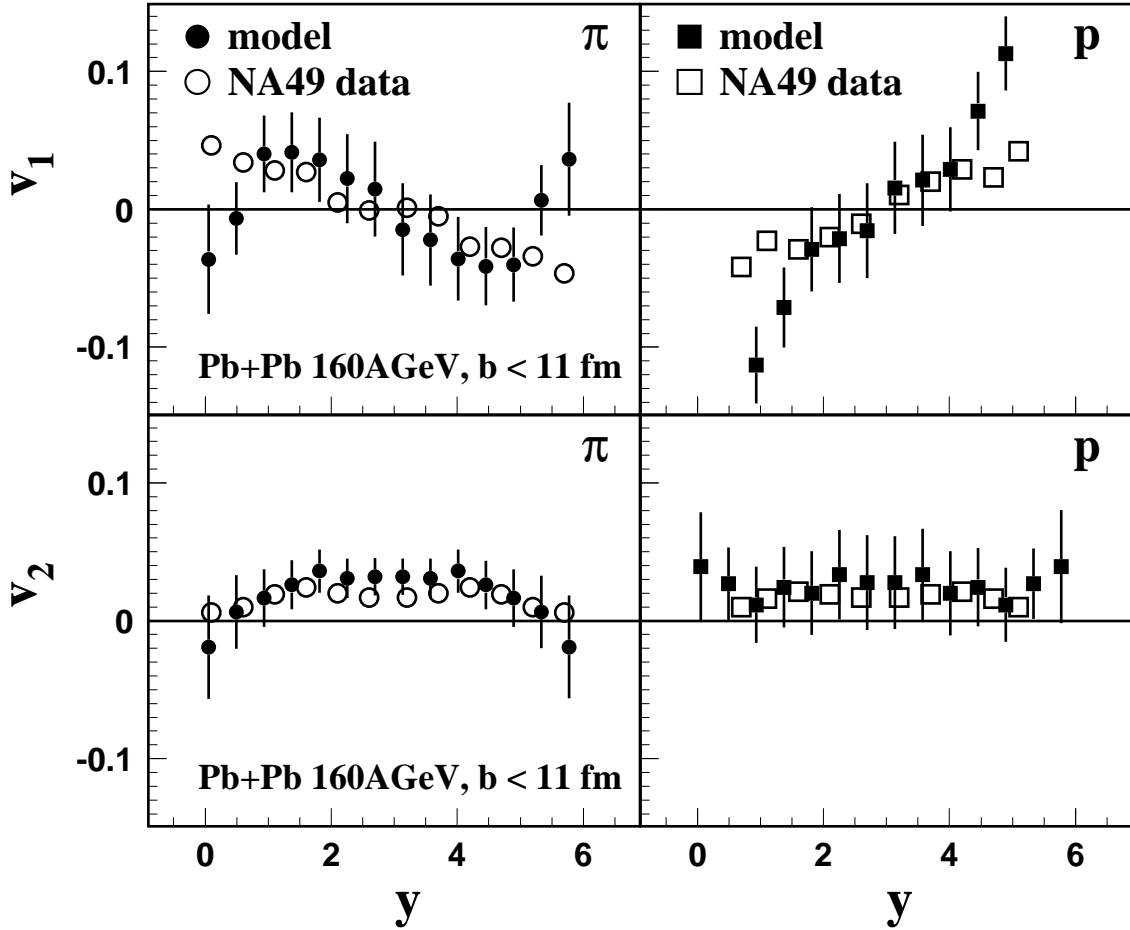


FIG. 2. Directed flow (upper row) and elliptic flow (lower row) for pions (left panels) and protons (right panels) in minimum bias Pb+Pb collisions at SPS energies. Solid symbols indicate microscopic calculations, open symbols show the experimental data taken from [24].

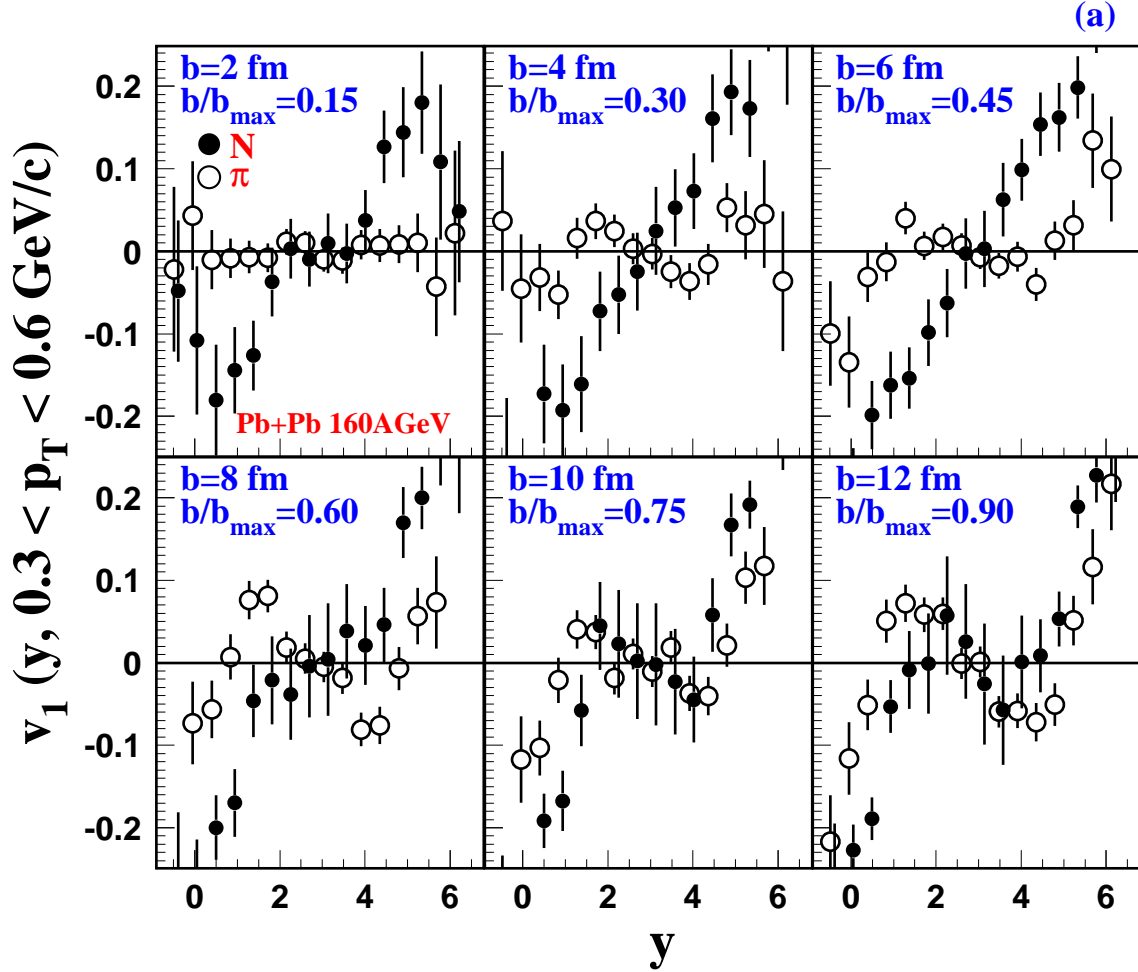
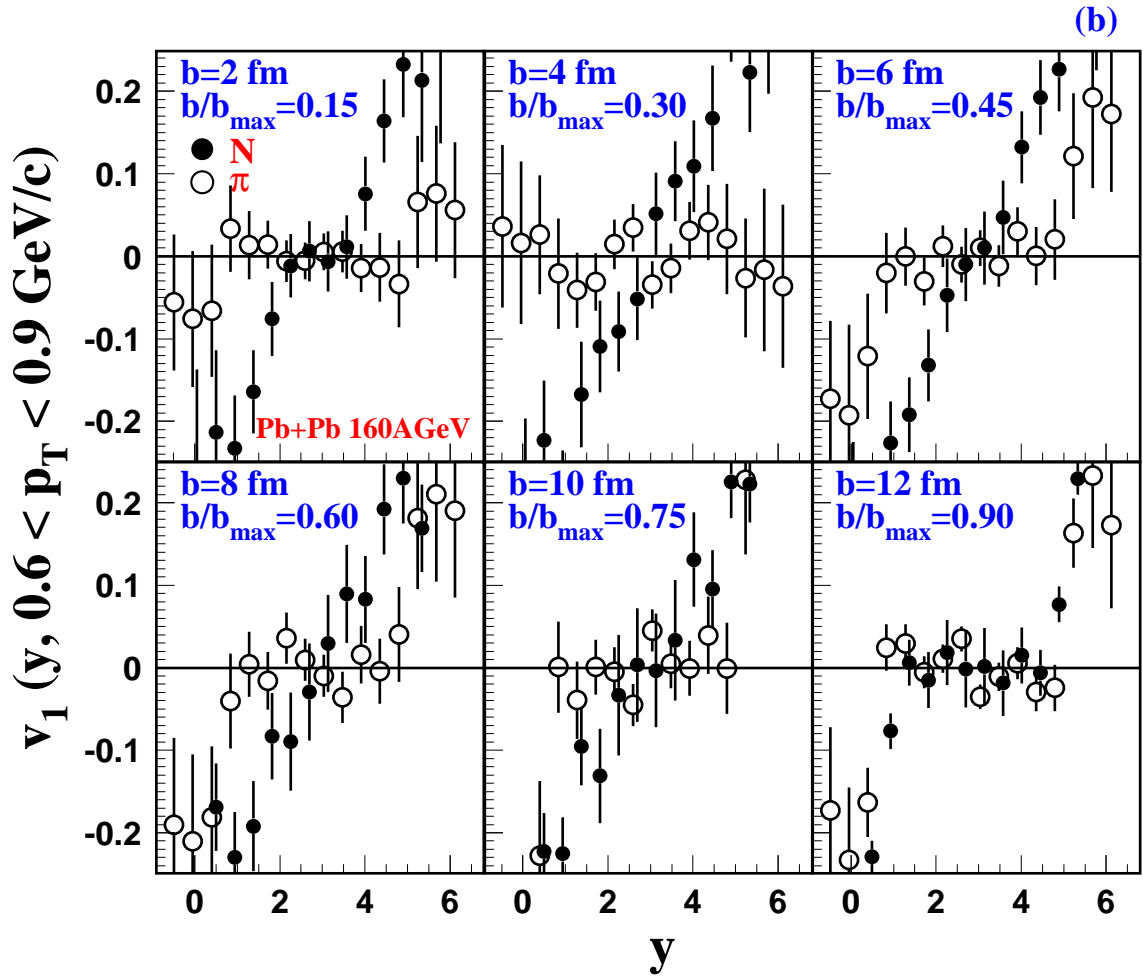


FIG. 3. (a) Centrality dependence of directed flow, $v_1(y, \Delta p_t)$, of nucleons (solid circles) and pions (open circles) in the transverse momentum interval $0.3 < p_t < 0.6$ GeV/ c in Pb+Pb collisions at 160A GeV.

(b) The same as (a) but for $0.6 < p_t < 0.9$ GeV/ c .



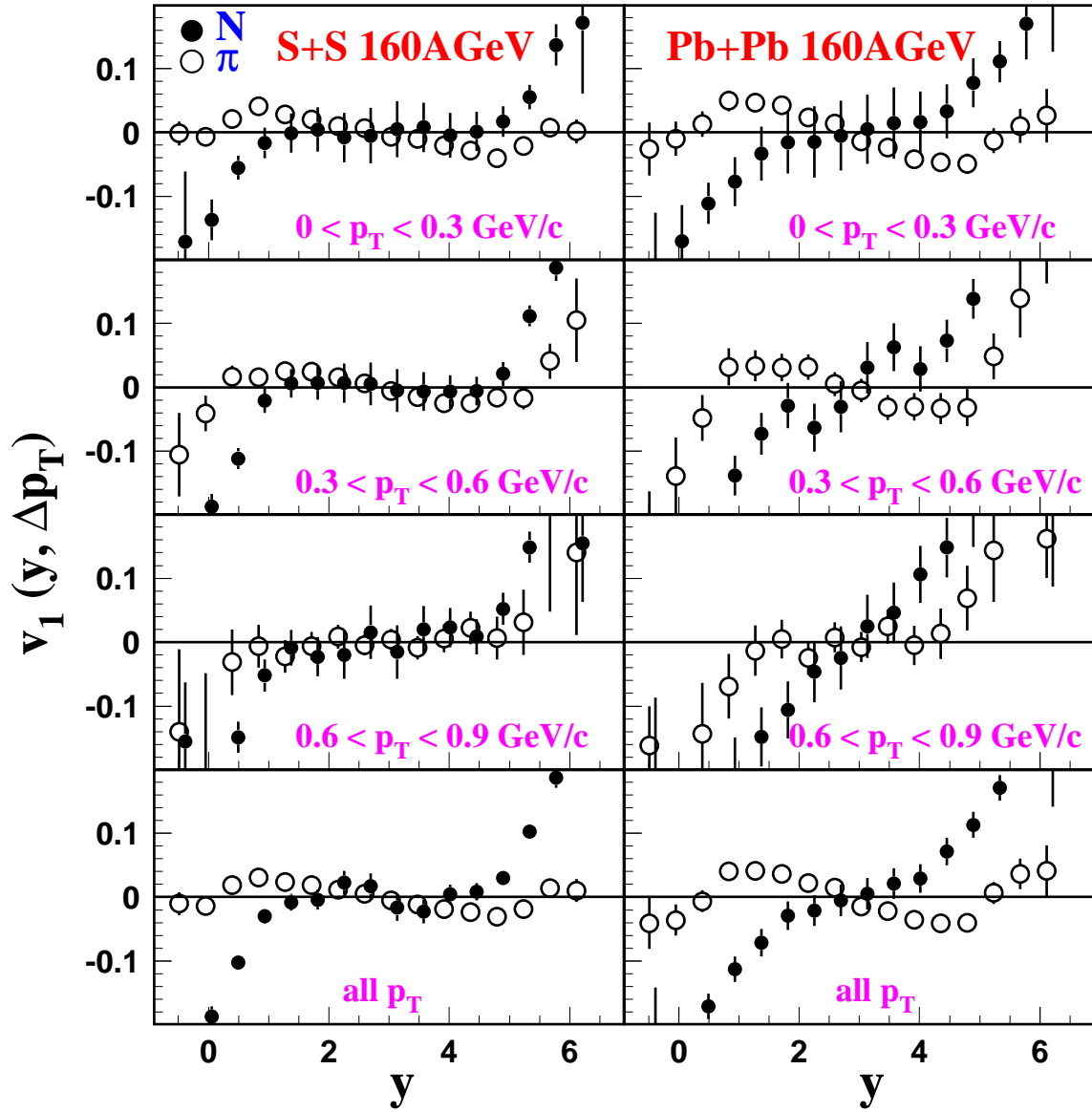


FIG. 4. Directed flow, $v_1(y, \Delta p_t)$, of pions (open circles) and nucleons (solid circles) in different p_t intervals in minimum bias S+S (left panels) and Pb+Pb (right panels) collisions at 160A GeV.

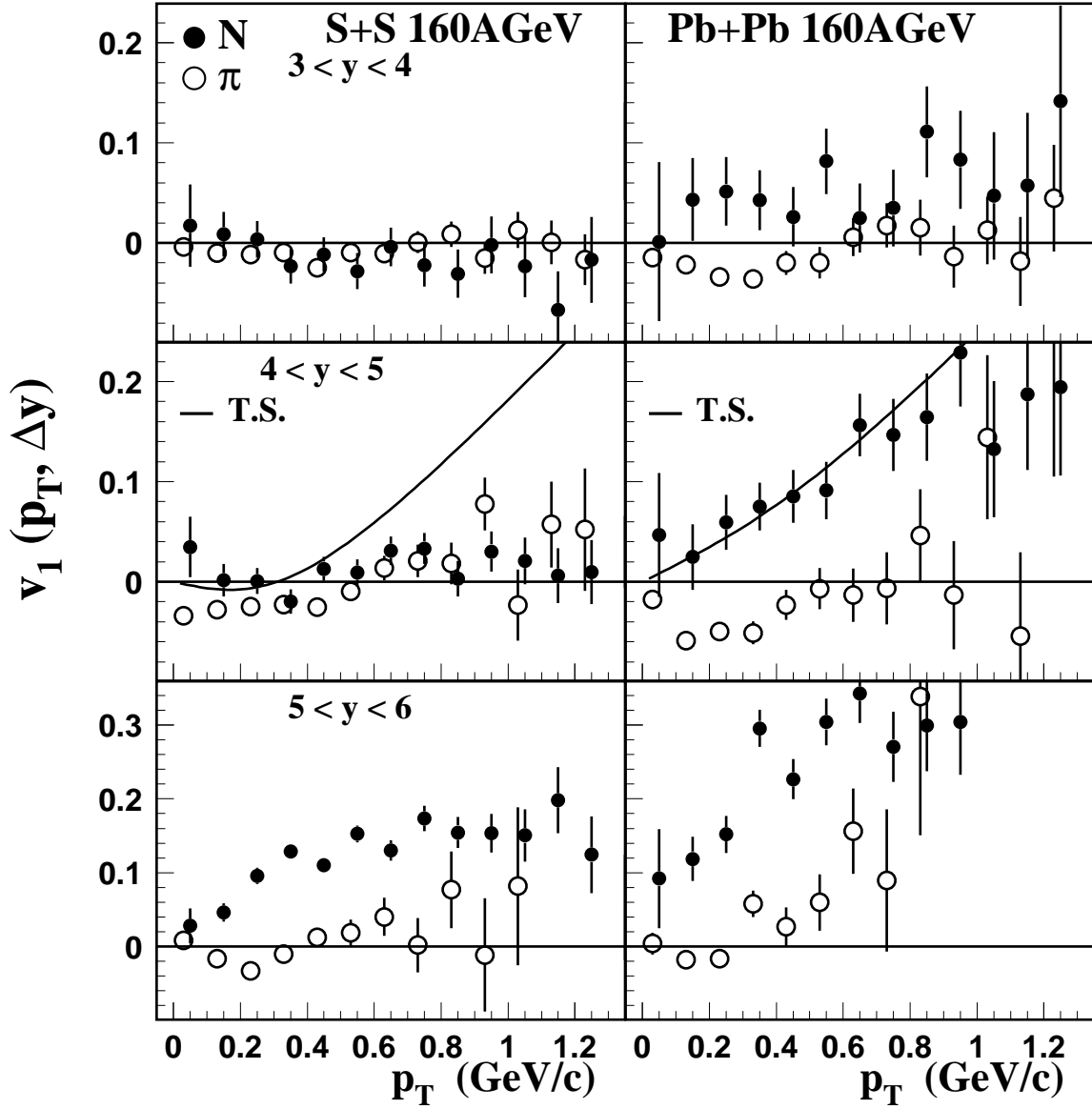


FIG. 5. Directed flow, $v_1(p_t, \Delta y)$, of pions (open circles) and nucleons (solid circles) in different rapidity intervals in minimum bias S+S (left panels) and Pb+Pb (right panels) collisions at 160A GeV. Solid curves indicate the results of the fit of Eq. (4) to the protons with $p_t \leq 0.45$ GeV/c in the rapidity interval $4 < y < 5$. See text for details.

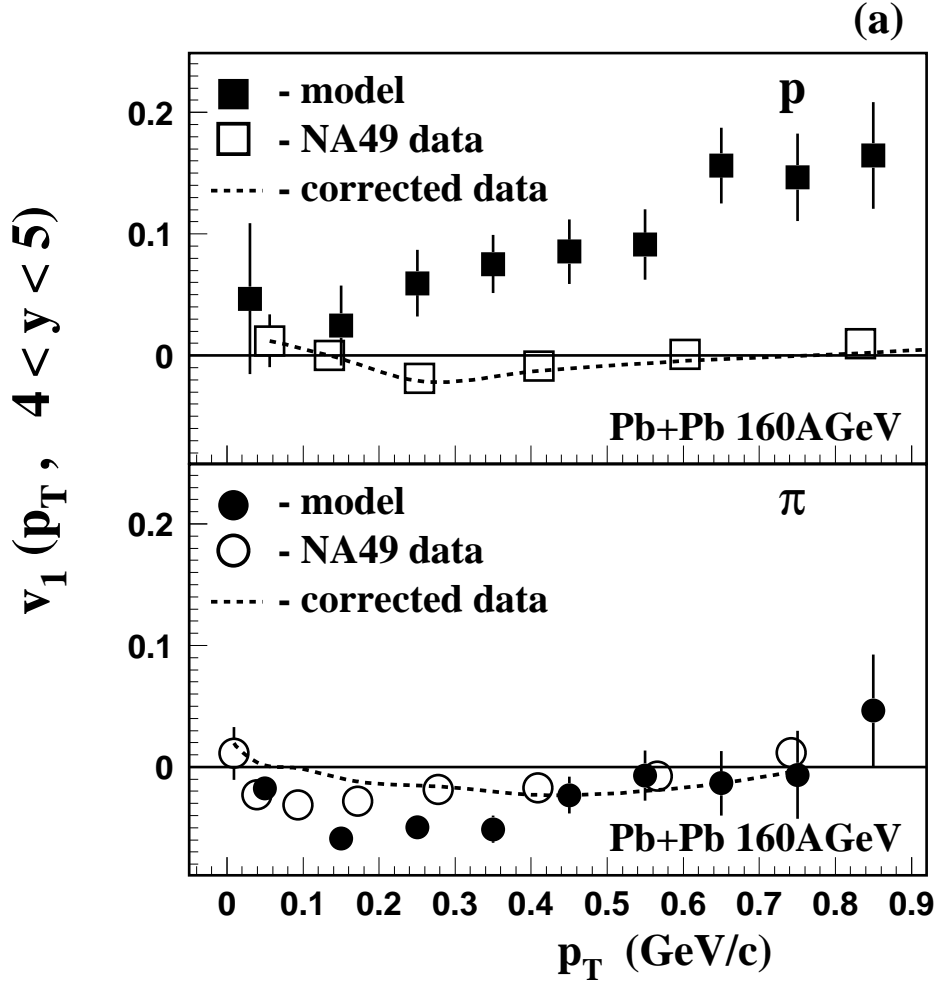


FIG. 6. (a) Directed flow, $v_1(p_t)$, of pions (open circles) and protons (solid circles) with the rapidity $4 < y < 5$ in Pb+Pb (upper panel) and S+S (lower panel) collisions at 160A GeV. Open and solid stars show the experimental results [23] on pion and proton directed flow, respectively. Dashed curves are the corrected data taken from [50]. (b) The same as Fig.6(a) but for protons with $y < 0.5$ in Pb+Pb collisions. Data (open squares) are taken from [26], solid squares indicate the model predictions.

